

BATCH-MICROFABRICATED ARRAYS OF ELECTROSPINNING EMITTERS FOR HIGH THROUGHPUT GENERATION OF NANOFIBERS

P. J. Ponce de Leon¹, F. A. Hill², and L. F. Velásquez-García²

¹Department of Mechanical Engineering, Massachusetts Institute of Technology, USA

²Microsystems Technology Laboratories, Massachusetts Institute of Technology, USA

Abstract: We report the design, fabrication, and experimental characterization of an externally-fed, silicon batch-fabricated MEMS electrospinning planar array with as many as 9 steady-operating emitters in 1 cm² – more than a 7-fold increase in emitter density compared to state-of-the-art MEMS multiplexed electrospinning sources. The device simultaneously generates multiple nanofiber jets at 20 kV or less bias voltage by using an array of pointed emitters that enhance the local electric field to trigger the ionization of the polymer solution at the emitter tips. The surface of the emitters is patterned with a microstructure that enables the delivery of polymer solution to the emitter tips without the need for external pumping. SEM images confirm fiber diameters on the order of 150 nm, which are comparable to those produced by other electrospinning techniques.

Keywords: electrospinning, multiplexed MEMS electrospray, nanofibers, nano-manufacturing.

INTRODUCTION

The fabrication of nanostructured materials with increased throughput and controlled morphology will enable the implementation of advanced energy storage and power conversion systems at low cost. Nanofibers are especially attractive for energy applications because their low dimensionality gives them unique properties. For example, dye-sensitized solar cells benefit from the reduction of grain boundaries associated with the 1D structure, which improves charge conduction. In addition, porous nanofiber mats allow for better infiltration of the viscous polymer gel containing the dye sensitizers [1]. Also, the high surface-to-volume ratio of nanofibers make nanofiber mats ideal scaffolds for catalyst dispersion in fuel cells [1].

Electrospinning refers to the technique to generate nanofibers using strong electric fields and polar, high molecular weight polymer solutions. A high enough electric field deforms the free surface of the liquid into a conical shape [2]. The apex of the cone emits a charged fiber that undergoes chaotic electrostatic whipping that stretches the fiber and greatly reduces its diameter. Electrospinning is the only known process that can generate nanofibers of arbitrary length with controlled morphology, and it has unmatched versatility as it can create non-woven/aligned mats of metallic, dielectric, and semiconducting fibers. However, the practical application of these nanofibers is limited to high-end products because of the very low throughput of standard electrospinning sources.

Increasing electrospinning throughput by multiplexing emission sources has been actively investigated for over a decade. Multiple-needle

approaches have been reported [3]; however, the size of the syringes limits the miniaturization of the array, and the complexity of the associated hydraulic network increases rapidly with the number of syringes. PDMS microfluidics can simplify fabrication of the hydraulic network, although miniaturization greatly increases the power required to pump a given flowrate and also increases the risk of clogging. In addition, reported MEMS PDMS-based electrospinning sources lack electric field enhancers at the emission sites [4] that would lower operational voltage. Free-surface electrospinning sources achieve relatively high throughput using no pumps, channels, or needles, but they require bias voltages on the order of 100kV at typical working distances to trigger the surface waves whose crests act as emission sites [5],[6]. Also, these sources exhibit inferior fiber uniformity and lack run-to-run repeatability. Near-field electrospinning (NFES) is a technique that employs significantly lower voltages applied over much smaller working distances in order to spin fibers in a more stable fashion, introducing the possibility of precise fiber deposition and denser, low-powered arrays [7].

In the current work, a hierarchically structured, externally-fed MEMS electrospinning array technology is demonstrated. Linear (i.e. 1D) arrays of meso-scale spikes, which serve as emitters, are assembled into a slotted base to form planar (i.e., 2D) arrays, as shown in Fig. 1. Micro-scale structures on the emitter surface enable the delivery of fluid to the field-enhancing spike-tips where it is spun into fibers. Using this technology, we implemented MEMS planar arrays with as many as 9 electrospinning emitters with 3mm pitch, which is less than half the pitch of state-of-the-art MEMS linear electrospinning arrays [4] and correlates to a 7-fold increase in area density.

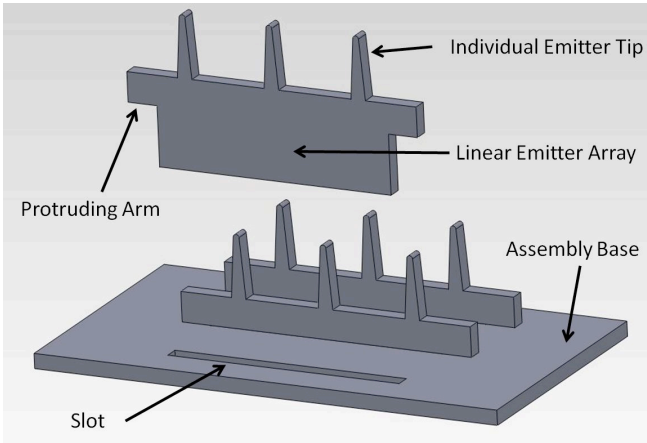


Fig. 1: Device schematic: three linear arrays are assembled into a slotted base to make a planar array.

DESIGN CONCEPT

Our MEMS multiplexed electrospinning source uses externally-fed emitters to circumvent the clogging and pumping problems that pressure-fed electrospinning sources have. In order to operate continuously, fluid must be replenished to the emitter tips from free-surface flow alone. Therefore, a hydrophilic emitter surface is required to enable fluid spreading. On a smooth surface, complete spreading can only be achieved with contact angles approaching zero, which are rare. However, for roughened surfaces, surface energy minimization relaxes the spreading condition to

$$\cos(\theta) \geq \cos(\theta_{crit}) = \frac{1-\varphi}{r-\varphi} \quad (1)$$

where the roughness r is defined as the ratio of actual area to apparent area and φ is the ratio of dry area to apparent area in the spreading region. For a roughness structure composed of hexagonally packed micropillars (Fig. 2), these quantities are easily calculated in terms of the diameter d , height h , and pitch p of the pillars. Capillary forces in these "micropillar forests" [8] can "hemi-wick" [9] liquid in a process that is analogous to capillary rise in a closed tube. The dynamics of hemi-wicking through the micropillar forest can be solved for numerically [10] or approximated using Darcy's Law. For the highly viscous solutions used in electrospinning, the dynamics are sufficiently slow that it is prudent to "prime" the emitters by coating them with polymer just prior to operation; this allows a liquid film to quickly impregnate the micropillars, which can then support a secondary film outside of the roughness [11]. Under the influence of the electric field, this secondary layer contributes significantly to overall fluid replenishment rate, allowing steady operation of the emitters.

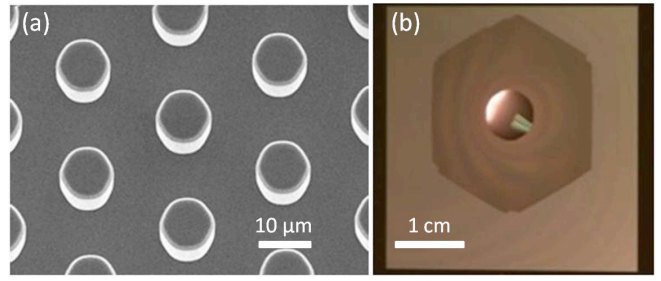


Fig. 2: a) Micropillar surface roughness and (b) hemi-wicking spread of a droplet through the roughness.

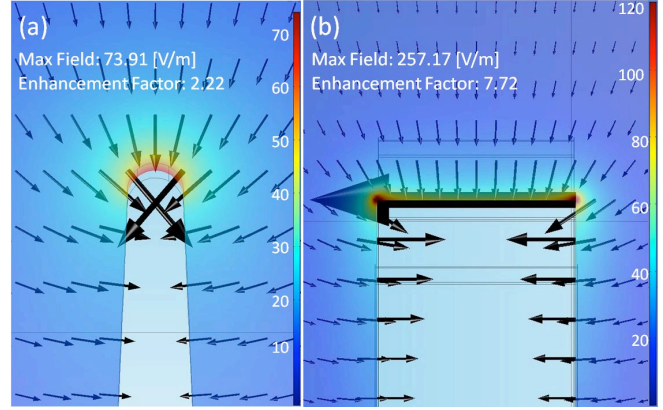


Fig. 3: Electric field simulation for 1V and 3 cm collector separation: (a) front view and (b) side view.

Our MEMS multiplexed electrospinning source uses high aspect ratio emitters that act as field enhancers to ionize the polymer solution at low voltage. The emitters trigger nanofiber generation when the electrostatic pressure surpasses the pulling due to surface tension, a condition given by

$$\frac{1}{2} \epsilon_o \cdot E_s^2 \geq \frac{2 \cdot \gamma}{R_c} \quad (2)$$

where ϵ_o is the electrical permittivity of free space, E_s is the electric field at the surface of the tip, γ is the surface tension of the liquid, and R_c is the radius of curvature of the liquid free surface, which is on the order of the tip radius. $E_s \approx \beta \cdot V$, where V is the bias voltage and β is the field factor; therefore, spikes with high field factor achieve ionization of the liquid with less voltage. For ideal spiked structures of length L and tip radius r , β should grow linearly with the aspect ratio L/r [12]. The spike tips of our MEMS multiplexed electrospinning source contain moderate curvature r in one direction and no curvature in the other direction except at the edges where the curvature is very high. COMSOL Multiphysics was used to simulate the electrostatics for this type of geometry and determine the field factor of the spike. The results reveal that the sharp edge curvature overpowers the

moderate curvature defined by the tip radius, such that variations in tip radius have only a minor effect on the field enhancement (Fig. 3). Therefore, it is expected that electrospinning of nanofibers will be concentrated at the sharp edge where the micropillar forest terminates.

FABRICATION

Our MEMS electrospinning emitter arrays are batch-microfabricated from 500 μm thick, 6-inch double side polished silicon wafers. We used deep reactive ion etching (DRIE) and a nested mask composed of a developed photoresist film on top of a reactive ion etching (RIE)-patterned silicon oxide film to etch the surface microstructure and extract the linear arrays of spikes from the silicon substrate. The resulting structure is shown in Fig. 4. The slotted base piece is also microfabricated using DRIE, with the slot widths tapered for a sliding interference fit so that assembly of the emitters can be achieved with mild force using a pair of tweezers. Good vertical alignment is maintained with protruding arms on the linear emitter arrays that contact the top of the base on both sides of the slot. A single linear emitter array has an active length of 1 cm with 1 to 5 emitters measuring 0.5-5 mm in height and 50-250 μm in tip radius. The micropillar surface roughness has pillars with 5-35 μm diameter, 20-40 μm pitch, and 100-200 μm height.

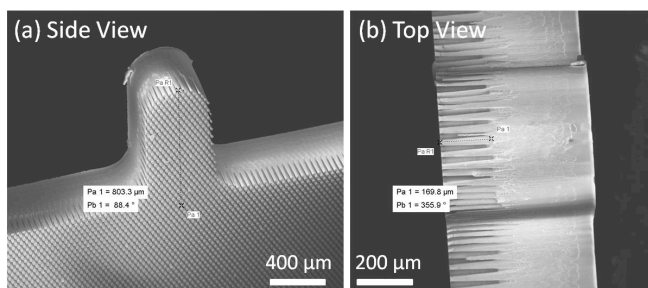


Fig. 4: SEM image of emitter tip: (a) side and (b) top views.

EXPERIMENTAL

Polyethylene oxide (PEO) with an average molecular weight of 600,000 g/mol was dissolved in deionized water at a concentration of 6% w/v. This solution was further diluted to yield concentrations between 2 and 6 w/v% in water/ethanol mixtures ranging from 100/0 v/v to 60/40 v/v. Assembled planar emitter arrays were secured with to a grounded electrical contact on a support rig made of polyphenylene sulfide (PPS) –a chemically resistant dielectric. DC high voltage was biased between the emitter array and a collector, which is placed between 1 and 15 cm away from the emitters (Fig. 5). Polymer

solution was deposited over the emitters with a pipette, and the voltage was increased until the initiation of fiber emission. Video images were recorded of full arrays and individual emitters during electrospinning to monitor the fiber production process.

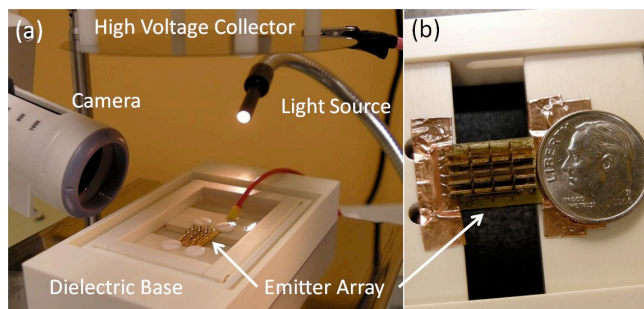


Fig. 5: a) Experimental setup and (b) array size compared with a dime.

DISCUSSION

Our devices demonstrate successful electrospinning of PEO nanofibers, like those in Fig. 6, with diameters of a few hundred nanometers or less. Electrospinning of higher concentration solutions with higher viscosity resulted in thicker, more uniform fibers. We also noted several different regimes of electrospinning, which seem to be determined by combinations of emitter-electrode geometry, wetting characteristics, and electric field strength. In all cases, the starting voltage for fiber emission proved to be greater than what was required to maintain electrospinning from already flowing jets, so in our tests we often lowered the voltage below the starting value once the process had initiated. In general, this resulted in more uniform, controlled emission.

In one emission regime observed for shorter, closely-packed emitters, mobile emission jets roam over the array area during the course of the electrospinning process. Jets occasionally pin to individual emitter tips, but do not stay anchored for long and also emit directly from the liquid free-surface. Electrospinning in this regime exhibits extensive chaotic whipping instability. Taller emitters are much better at anchoring emission jets to the emitter tips, and they turn on at lower voltages due to stronger electric field enhancement. Fig. 7a shows an array of nine 5 mm-tall emitters, each generating one or more jets from its tip; they are also able to support Taylor cones typical of traditional needle electrospinning sources that produce initially wider fibers (Fig. 7b) that narrow due to whipping on their way to the collector. This regime is characterized by chaotic electrostatic whipping instability, but offers more control due to the improved jet anchoring.

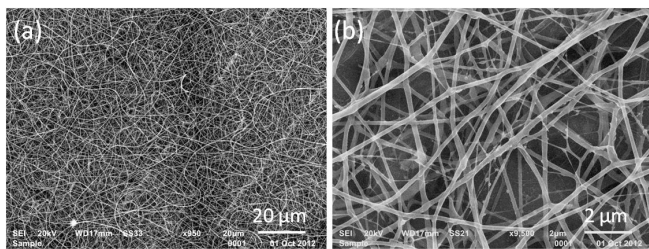


Fig. 6: Unwoven nanofiber mat at (a) low magnification and (b) high magnification.

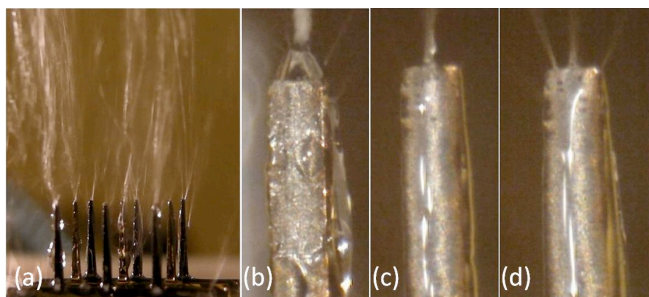


Fig. 7: a) 3×3 Array of 5 mm-tall emitters. (b) Larger Taylor cone with wider jet. (c) Single and (d) multiple fiber emission anchored at tips.

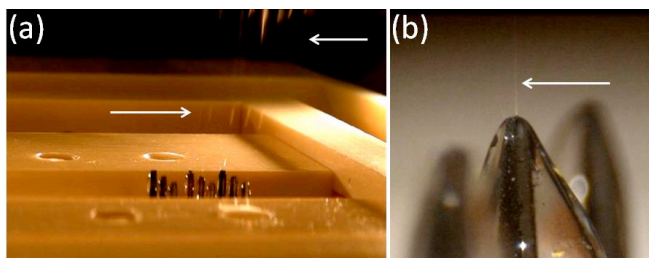


Fig. 8: a) Stable emission from 5 mm-tall emitters. (b) Emission of extremely fine initial jet.

The 5 mm-tall electrospinning emitters can also support a more stable regime of emission at shorter working distances and lower voltages. However, such emission is more difficult to maintain, especially uniformly across the array. It is highly sensitive, not only to the operating voltage and electrode alignment but to the specific electric field profile as influenced by surrounding objects. Sometimes the strong field-enhancement characteristic of shorter working distances produces a corona discharge, which seems to inhibit electrospinning. Fig. 8a captures stable emission from a 5 mm-tall array that sits in a bath of polymer solution and is partially shielded by the dielectric base. Only part of the array actually emits fibers, but they are finer upon emission (Fig. 8b) and therefore, they require less whipping and stretching to reach desirable diameters. For an identical solution of 2.8% w/v PEO in 60/40 ethanol/water spun from 5mm spikes, a sample of chaotically whipped fibers had an average diameter of 166 nm while a sample of stable

fibers averaged 209 nm. If such narrow fibers can be reliably produced without whipping, this can minimize jet-to-jet interaction and greatly increase the density with which emitters may be packed. Future work will look at integrating a finely-aligned, proximal extractor electrode to explore this idea.

ACKNOWLEDGEMENT

This work was supported by the Defense Advance Research Projects Agency Microsystems Technology Office (DARPA/MTO) under contract W31P4Q-11-1-0007 (program manager J. Judy). Any opinions, findings, and conclusions or recommendations expressed in this publication are those of the authors and do not necessarily reflect the views of the US Government and therefore, no official endorsement of the US Government should be inferred.

REFERENCES

- [1] Thavasi V., Singh G., Ramakrishna S. 2008 Electrospun Nanofibers in Energy and Environmental Applications *Energy Environ. Sci.* **1** 205-221
- [2] Taylor G. I. 1964 Disintegration of Water Drops in an Electric Field *Proc. R. Soc. London A* **280**
- [3] Theron S. A., Yarin A. L., Zussman E., Kroll E. 2005 Multiple jets in electrospinning: experiment and modeling *Polymer* **46** 2889-2899
- [4] Srivastava Y., Marquez M., Thorsen T. 2007 Multijet Electrospinning of Conducting Nanofibers from Microfluidic Manifolds *J. Appl. Polym. Sci.* **106** 3171-3178
- [5] Petrik S., Maly M. 2009 Production Nozzle-Less Electrospinning Nanofiber Technology *MRS Proceedings*, **1240** 1240-WW03-07 doi:10.1557/PROC-1240-WW03-07
- [6] Lukas D., Sarkar A., Pokorny P. 2008 Self-organization of jets in electrospinning from free liquid surface: A generalized approach *J. Appl. Phys.* **103** 084309
- [7] Chang C., Limkrailassiri K., Lin L. 2008 Continuous near-field electrospinning for large area deposition of orderly nanofiber patterns *Appl. Phys. Lett.* **93** 123111
- [8] Ishino C., Reyssat M., Reyssat E., Okumura K., Quéré D. 2007 Wicking within forests of micropillars *Europhysics Letters* **79** 56005
- [9] Quéré D. 2008 Wetting and Roughness *Annu. Rev. Mater. Res.* **38** 71-99
- [10] Xiao R., Enright R., Wang E. N. 2010 Prediction and Optimization of Liquid Propagation in Micropillar Arrays *Langmuir* **26** 15070-15075
- [11] Seiwert J., Clanet C., Quéré D. 2011 Coating of a textured solid *J. Fluid Mech.* **669** 55
- [12] Podenok S., Sveningsson M., Hansen K., Campbell E. E. B. 2006 Electric Field Enhancement Factors Around a Metallic, End-Capped Cylinder *NANO* **01** 87-93